Hydrodynamic Cleaning of a Viscous Film From the Inside of a Long Tube

Elizabeth S. Mickaily and Stanley Middleman
Dept. of AMES/Chemical Engineering, The University of California, San Diego, La Jolla, CA 92093

A simple fluid dynamic model is developed which predicts the thinning rate of a viscous film of liquid, in contact with the smooth interior surface of a long cylindrical tube, due to the shearing action of a turbulent flow of an immiscible fluid through the tube. Experiments indicate the degree to which the model provides an accurate means of predicting viscous film removal from the tube. Similar experiments performed with electrochemically roughened tubes elucidate the limitation of this cleaning process due to surface roughness. The observed limitation is consistent with an analysis based on numerical solutions of the equations for shear flow over a rough surface.

Introduction

As part of an ongoing study of cleaning technology we are interested in the mechanics of removal of liquid films adherent to solid surfaces. Earlier works (Klepikov and Kamener, 1971; Yeckel and Middleman, 1987; Yeckel et al., 1990) have focused on localized cleaning through the use of high-speed liquid jets which impinge on the contaminant film and remove the contaminant by inducing flow, generally through a combination of pressure and viscous shearing forces. In this study, we have examined the removal of the liquids from the interior of long tubes, particularly the issue of what occurs when the oil film is thinned to the level of microscale surface roughness.

The hydrodynamics of the removal of thin films of liquid contaminants from surfaces is of considerable intellectual and industrial interest. From an intellectual standpoint, it is a problem that requires knowledge and application of concepts of fluid dynamics, surface chemistry and tribology. An understanding of hydrodynamic cleaning also sheds light on related problems such as coating flows (Middleman, 1987; Sullivan et al., 1987), retention of lubricant on a rotating magnetic storage disk (Strong and Middleman, 1989), the ability of a lubricant to retard the impending collision of a pair of approaching surfaces, and convective mass transfer to and from cavities (Sullivan and Middleman, 1985; Alkire, 1990; Higdon, 1990).

From an industrial viewpoint, the information gained from this study is important as well. In various industrial settings, tubing used to convey a liquid through a process or, between reservoirs of a system, may need to be cleaned periodically to the extent that essentially no residual liquid remains adhering to the inside surface of the tube. While the use of an appropriate solvent is the most common means of cleaning the tubing, typically by continuous flushing with the solvent, this method has some serious limitations. One lies in the expense of the solvent, and/or the subsequent expense of separation of the contaminant from the solvent, and the recovery of the solvent for recycling. Another limitation lies in the potential environmental harm if the solvent is released to the environment external to the process.

The solvent issue is a serious one, and it is a key factor that motivates this study. In the aerospace industry, for example, tubing used to convey fuel to engines must satisfy stringent conditions on the removal of residual oil films deposited during the manufacturing of the tubing. Current practice involves flushing of the tubes with trichloroethane (TCA), a solvent that is scheduled to be phased out under the Montreal Protocol because of its potential adverse environmental effects (Wolf, 1989; Evanoff, 1990). While a search is in progress for replacement solvents, the question of the degree to which these films may be removed *without any solvent* has been raised. Specifically, the fundamental work described here supports the idea that low levels of residual oil can be achieved by the flushing action of an immiscible fluid and investigates the efficiency with which *hydrodynamic shear* can remove an adherent layer of a second immiscible fluid from the inside surface of a tube.

Theory: a Cleaning Model

Figure 1 shows the situation of interest. A long tube of

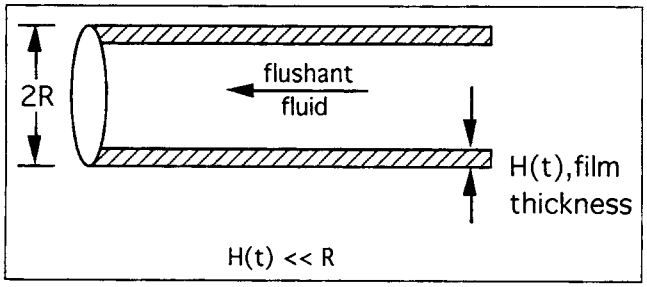

Figure 1. Tube with thin uniform film inside.

uniform circular cross section is contaminated with a thin, uniform film of a liquid. By the qualifier "thin" we imply that the film thickness $H(t)$ always satisfies $H(t) << R$. The oil film is being constantly sheared by a turbulent immiscible flushant fluid, which in turn causes a shear flow in the film. Pressure effects, which can aid the shear flow in the film, have been shown to be of order H/R with respect to the shear flow, and thus small for film thicknesses much less than the tube radius (Mickaily, 1992). Locally, the average velocity V_f in the oil film, assuming a thin-film exhibiting planar Couette flow, is:

$$V_f = \frac{V_s}{2} \tag{1}$$

where the velocity at the oil/flushant interface V_s is given by the shear stress relation:

$$\tau_o = \mu_{\text{oil}} V_s / H \tag{2}$$

We can find the shear stress τ_o from the definition of the friction factor for the flushant fluid:

$$f = \frac{\tau_o}{\frac{1}{2}\rho[Q/\pi R^2]^2} \tag{3}$$

where ρ is the density of the flushant, Q is the flushant flow rate, and R is the radius of the tube being cleaned.

A local mass balance on the oil film shows that the transient film thickness is a function of axial position:

$$\frac{\partial H}{\partial t} + \frac{\partial q}{\partial z} = 0 \tag{4}$$

where q is the volume flow rate (per unit width) within the contaminant film. If we assume that the flow in the contaminant film is locally planar Couette flow, then

$$q = \frac{1}{2} V_s H(z,t) = \frac{H^2(z,t)\tau_o}{2\mu_{\text{oil}}} \tag{5}$$

Hence, H satisfies a partial differential equation of the form:

$$\frac{\tau_o}{\mu_{\text{oil}}} H(z,t) \frac{\partial H}{\partial z} = -\frac{\partial H}{\partial t} \tag{6}$$

While this differential equation admits an explicit analytical solution ($H = \mu_{\text{oil}} z/\tau_o\, t$), it is not a solution that satisfies physically meaningful boundary and initial conditions. The general solution to Eq. 6, from the method of characteristics, may be written in the form:

$$H(t) = f\left(z - \frac{\tau_o}{\mu_{\text{oil}}} Ht\right) \tag{7}$$

where f is an unknown function. Physically, as well as mathematically, the behavior of the solution at the entrance $z = 0$ is propagated downstream to affect the film thickness at the end of the tube. Depending on the wetting characteristics of the contaminant film, the entrance region may at some time become free of the film, and a three-phase contact line then moves downstream toward the tube exit. The physics of such a flow is very complex, and its analysis is well beyond the scope of this study.

We turn instead to an approximate analysis that suggests an empirical equation that can be tested against data for removal of the contaminant film. In view of the fact that we will measure the average $\bar{H}(t)$ in our experiments, we first average Eq. 4 over the tube length L as follows:

$$\int_0^L \frac{\partial H}{\partial t}\, dz = -\int_{q_0}^{q_L} dq \tag{8}$$

Then

$$\frac{d}{dt}\int_0^L H\, dz = q_o - q_L$$

or

$$L\frac{d\bar{H}}{dt} = -q_L = \frac{-\tau_o H_L^2}{2\mu_{\text{oil}}} \tag{9}$$

We have used the fact that no contaminant fluid enters the tube, so $q_o = 0$. Equation 9 is a simple ordinary differential equation for the average film thickness, but its solution requires a value for the downstream film thickness, H_L. Since this parameter is itself unknown, we will solve Eq. 9 by first finding an approximation for H_L.

The approximation procedure begins with the assumption that the film thickness is everywhere uniform along the z-axis of the tube. (Of course, this approximation is inconsistent with Eq. 4.) Then an oil balance gives:

$$V_f 2\pi RH = -2\pi RL\, dH/dt \tag{10}$$

where H is the (assumed uniform) film thickness at any time. The introduction of Eqs. 1 and 2 into Eq. 10 yields:

$$-\frac{dH}{dt} = \frac{H}{2L} V_s = \frac{H}{2L}\frac{\tau_o H}{\mu_{\text{oil}}} \tag{11}$$

or

$$\frac{d\left(\frac{1}{H}\right)}{dt} = \frac{\tau_o}{2L\mu_{\text{oil}}} \tag{12}$$

Now, we rewrite Eq. 6 in the form:

$$\frac{1}{H}\frac{\partial H}{\partial z}=\frac{\mu_{oil}}{\tau_o}\frac{\partial}{\partial t}\left(\frac{1}{H}\right)=\frac{1}{2L} \tag{13}$$

This has the solution:

$$\ln\left(\frac{H}{H_L}\right)=\frac{1}{2L}\,(z-L) \tag{14}$$

or

$$\frac{H}{H_L}=e^{-1/2}e^{z/2L} \tag{15}$$

The average of H then follows from:

$$\frac{\overline{H}}{H_L}=e^{-1/2}\int_0^1 e^{z/2L}d\left(\frac{z}{L}\right)=0.787 \tag{16}$$

or

$$H_L=1.27\overline{H} \tag{17}$$

Returning to Eq. 9 we may now write:

$$\frac{d\overline{H}}{dt}=\frac{-0.807\tau_o\overline{H}^2}{\mu_{oil}L} \tag{18}$$

We find finally,

$$\frac{H_o}{\overline{H}}-1=\frac{0.807\tau_o H_o}{\mu_{oil}L}\,t$$

or

$$\frac{1}{\epsilon}-1=0.807t^* \tag{19}$$

where H_o is the initial film thickness, t^* is a dimensionless flushing time variable, and

$$\epsilon\equiv\frac{\overline{H}}{H_o} \tag{20}$$

is the fractional reduction in the average film thickness. At this point, we have a testable model. The numerical coefficient given in Eq. 19 (0.807) is approximate. Hence, we will test the model by plotting our data in the form $(1/\epsilon-1)$ vs. t^*.

To calculate a value for t^* it is necessary to have a value for the shear stress τ_o. The shear stress averaged over the tube length could be measured indirectly from data on the pressure drop, using $\tau_o=R\Delta P/4L$. No such measurements were made. Instead, a friction factor plot for smooth tubes was used to produce a nominal value of τ_o for each flow rate. This procedure implies a belief that the oil-contaminated tubes exhibit pressure drops similar to smooth tubes at the same flow rates. The data reported here were obtained under conditions that the initial film thickness was at least an order of magnitude less than that of the tube radius. Hence, as cleaning proceeded to low levels of residual contaminant, the film thickness was several orders of magnitude less than the tube radius. While the potential for the oil-flushant interface to be roughened from surface instabilities exists, we expect that the level of roughness would be of the order of the film thickness at most, which, in turn, is much less than the tube radius. Hence, we assumed that the smooth tube friction factor correlation would provide a good estimate of the shear stress. As described later, the bare-tube roughness was itself very small (even for the so-called roughened tubes).

A consequence of our failure to provide measured values of τ_o is that any deviation between the model given in Eq. 19 and the data reflects not only the level of approximation of the assumed physics of the flow in the film, but also the use of an approximate value for the shear stress driving the contaminant from the tube.

Experimental Procedure

A series of experiments was carried out to test the model given in Eq. 19. Light-weight aluminum tubes, 22.8 cm in length with radii of 0.2 and 0.28 cm, were used. Each tube was initially cleaned in a xylenes/methanol solution in an ultrasonic cleaning device for about 3–4 minutes to ensure initial cleanliness of the internal tube surface. (Tubes were always handled with polyvinyl-gloved hands to prevent contamination from skin oils.) The tube was then dried using a soft paper towel for the external surface and dry, oil-free air for the internal surface. When dry, the tube was weighed to determine its clean, dry initial weight. The interior of the tube was then coated with a layer of either castor or olive oil as the contaminant film. (See Table 1 for oil properties.) This was achieved by filling an eye dropper with the selected oil and dripping several drops through one end of the tube. The oil was allowed to go through until it came out of the bottom, at which point the tube was inverted and the process repeated with the formerly bottom end of the tube up. In this way, a layer of oil was created on the inside tube surface. The inside of the coated tube was then blown with clean, dry air through each end for a few seconds to ensure a uniform oil coating. This step is important since the model is based on the removal of an assumed initially uniform oil film. Finally, the aluminum tube is weighed again (with the oil coating on the inner surface) as a measure of the initial film thickness.

With these preliminary procedures completed, the tube was placed in the experimental setup depicted in Figure 2. Air (used as the immiscible cleaning fluid) was obtained from a laboratory air tap. This tap was connected to a pressure regulator in series with a trap for residual oil coming in through the air

Table 1. Oil Properties Measured at 23°C (Lab-Room Temperature)

	Castor Oil	Olive Oil
μ_{oil}	700 cp	74 cp
ρ_{oil}	0.97 g/cm^3	0.92 g/cm^3
σ (in air)	35 dyne/cm	35 dyne/cm
θ_c (on Al.)	~0	~0

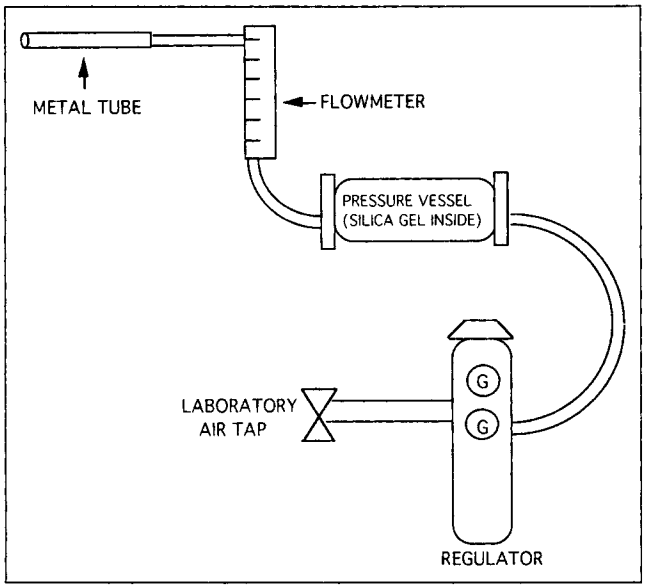

Figure 2. Experimental setup for oil removal using air.

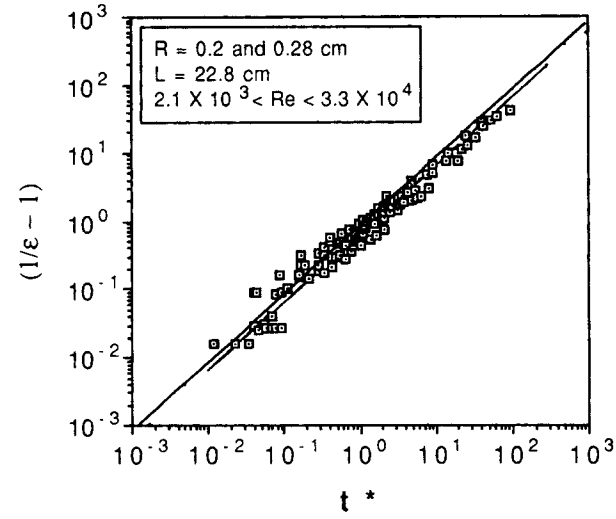

Figure 3. Combined short-time data for the removal of castor and olive oils from the inside of a straight aluminum tube using air as flushant.

pipe lines. The regulator was then connected to a pressure vessel containing silica gel which serves to trap any additional moisture remaining in the air flow. This desiccant chamber was in turn joined to an air flowmeter which was finally connected to the oil-coated tube to be cleaned. The air exiting the tube impinged on the bulb of a Fenske viscometer containing the selected oil. This final step allowed the oil in the bulb to be kept at approximately the same temperature as that of the air flushant and the oil film in the tube. In this way, accurate oil viscosity measurements could be made periodically during the experiment. Apparatus connections were made using short pieces of latex tubing (or thick-walled tubing where needed) and were secured with hose clamps. Although the initial films were thin (on the order of 10^{-3} cm), it is noted that the tube samples were always placed horizontally throughout the procedure to minimize gravity or drainage effects.

Now, air flow was turned on, and the flow rate was kept constant, within the turbulent range for a timed interval. Normally, the experiments were run until some visible amount of oil emerged from the free end of the tube. At this point, the sample tube was removed from the system, the oil rejected from the tube end was carefully tissue-wiped, and the tube was weighed. This timed cleaning/wiping/weighing procedure was repeated until no more cleaning was achieved, always taking care to keep the air flow at the *same* constant, turbulent rate. Each experiment was continually carried out over the course of 3 to 4 days.

The average film thickness at any point in time $\overline{H}(t)$ is given by:

$$\overline{H}(t) = (\text{mass of oil film at time } t)/(2\pi RL\rho_{\text{oil}}) \qquad (21)$$

All weighing was performed on a high precision, five-digit accuracy Sartorius 1712 MP8 balance.

Results and Comparison to Theory

To examine the validity of the theory, the experiment described above was performed several times for the two oils noted, using two different tube radii and a variety of turbulent Reynolds numbers in the range of $2.1 \times 10^3 < Re < 3.3 < 10^4$. The data (116 measurements) are plotted on logarithmic coordinates (Figure 3) to test Eq. 19. A least-squares line of the form of Eq. 19 yields a correlation coefficient (R^2) of 0.97, when the coefficient (0.807) is replaced with the value 0.59.

When the cleaning process is continued for long times, that is, past a t^* of about 50 or film thicknesses of about 10^{-5} cm (see Figure 4), the data appear to level off at a value of $(1/\epsilon - 1)$ approximately equal to 55 (corresponding to 98% cleaning). Thus, it would seem that no more oil can be removed past a cleaning limit of 98%, at which point the model is no longer valid. It was expected that the theory would fail at some point. Some of the possible reasons for this failure will be assessed in the next section.

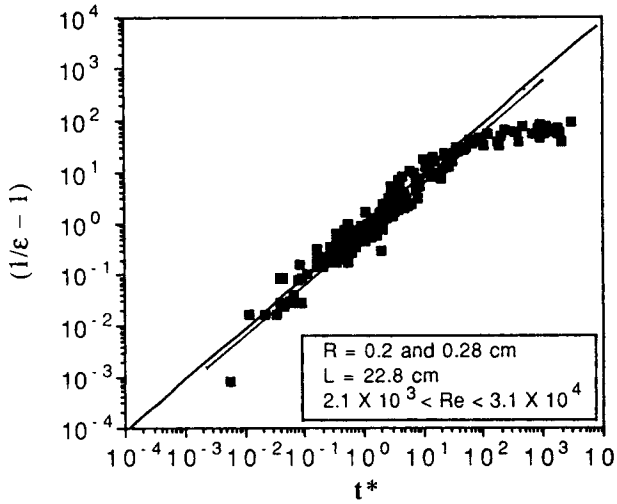

Figure 4. Combined long-time results for the removal of castor and olive oils using air as flushant.

Interpretation of Results

A major assumption of the model developed here is that the contaminant film has a smooth interface with the flushant, with a slowly varying film thickness in the axial direction. It is further assumed that the magnitude of the film thickness is small in comparison to the tube radius. These assumptions are essential to the use of a constant shear stress τ_o in relating the effect of the core flow on the contaminant film flow. Film instability is a potential issue and has been shown to exist for ultrathin films where van der Waals forces are the only stabilizing factors (Ruckenstein and Jain, 1973; Sharma and Ruckenstein, 1984). However, van der Waals forces only begin to dominate viscous and capillarity forces for films on the order of atomic dimensions (that is, tens to hundreds of Angstroms), a fact supported by the works of Teletzke et al. (1986), Israelachvili and Kott (1989), and Strong and Middleman (1989). Our final film thicknesses of about 1,000 Å are certainly thicker than atomic dimensions.

The stability of interior annular coatings has been studied by Goren (1962) for isolated films, and for core-annular flows (Joseph et al., 1984; Preziosi et al., 1989; Hu and Joseph, 1989; Papageorgiou et al., 1990) where the dynamics of the core flow induces instability in the annular film. A few oil cleaning experiments were performed during the course of this study using glass tubes and dyed silicon oil as the contaminant. In this way, instabilities could be observed visually. A wavelike pattern was noted, consisting of rings of alternating thick and thin fluid regions. Nonetheless, the pattern itself was uniform and moved at a rate consistent with that of the shearing flushant. Thus, for the purposes of our theoretical model of film removal, we assume that the shear stress acts "globally" on the film, regardless of instabilities, and that the shear stress (friction factor) relation for flow through a smooth tube should be valid for thin films, that is, for $H << R$.

One possible reason for the breakdown of the theory is the existence of a rough *solid* surface. Specifically, the idea is that when the film thickness is on the order of the surface roughness, fluid becomes trapped within the rough "architecture" of the surface (Higdon, 1985; Pozrikidis, 1987; Yeckel et al., 1990; Mickaily et al., 1992). Pursuing this idea, we chose to calculate the observed limiting film thickness (corresponding to the maximum 98% oil removal) and to compare it to the magnitude of the surface roughness.

For all of the experiments performed, the order of magnitude of the final film thickness was 10^{-5} cm (or 1,000 Å). Using a Bendix QB-type profilometer with a LK2-1520 probe, we were able to perform roughness measurements on the inside surface of the cylindrical tubes used. An average surface roughness amplitude of 7.6×10^{-6} cm (or 760 Å), which is of the order of the final film thickness, was obtained. Thus, we speculate that surface roughness is the primary factor hindering the continued cleaning that would be predicted by the theoretical model. This idea will be developed in the subsequent sections.

Experimental Tube Roughening Procedure

To explore the limitations of the cleaning experiments described earlier, an experiment was designed to study the effects of microscale surface roughness on fluid flow. The first step is to create rough aluminum metal tubes of the type described above. The roughening procedure is based on the electrochemical tunnel etching technique described by Alwitt et al. (1984). It is important to note, however, that their specimens consisted of high-grade, 0-temper, 99.99% aluminum foil fabricated to have high cubicity texture. This was essential for their purposes as they were interested in obtaining a highly uniform dispersion of tunnels in the (100) plane. The purpose here, however, is simply to provide moderately uniform tube roughening on a microscopic scale. The roughening procedure is detailed below.

Electrical leads were duct-taped near the top and bottom end of each metal tube to ensure even etching. Then, each tube was painted thoroughly on the outside with a thick layer of Microshield "stop-off lacquer" in an effort to prevent etching of the outside tube surface (and potentially to prevent total perforation of the metal). Care was taken to completely cover the electrical leads as well with the lacquer. The lacquer was allowed to dry over the course of one to two days. Once dry, the sample was cleaned for 10 minutes in a 1N NaOH solution at room temperature, and was then rinsed with deionized water and immediately placed in the apparatus depicted in Figure 5. The experimental setup consists of a large water bath maintained at a temperature of approximately 90°C. Within the water bath is a second reservoir holding a solution of 1N HCl. A power supply provides current to the anode, and the current is measured by an ammeter.

The aluminum tube sample to be etched was connected to the anodic lead, and a sample of aluminum foil acting as the cathode was placed at the opposite electrode. The aluminum foil was cut to have 2 to 3 times the surface area of the tube to be etched, thus preventing limited etching of the actual sample. Both specimens were completely immersed in the HCl solution, and a current density of 50 mA/cm^2 was supplied and held constant for a timed interval. The sample and aluminum foil were then immediately removed from the HCl and rinsed with deionized water. This entire procedure was performed for two aluminum tubes, each having an etchable (in-

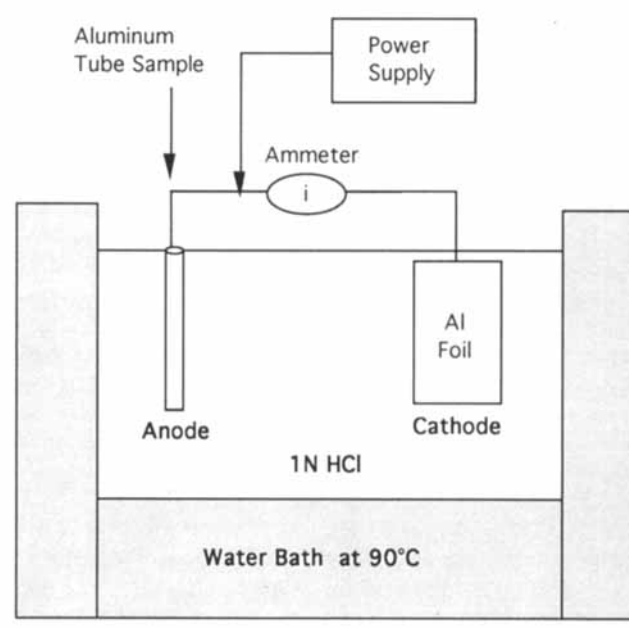

Figure 5. Experimental setup for tunnel etching of aluminum metal tubes.

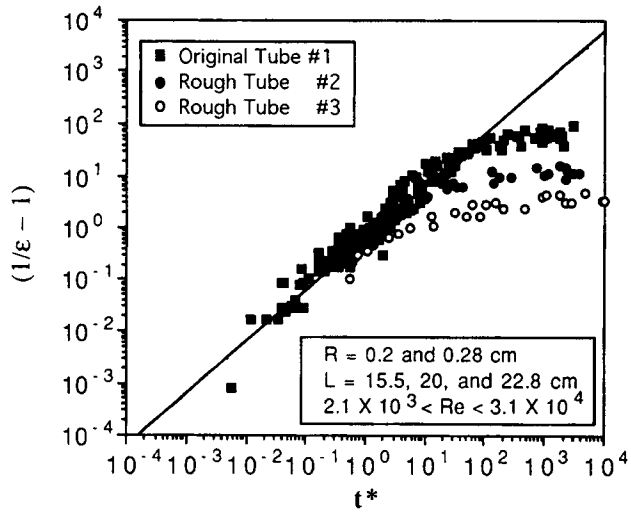

Figure 6. Combined data for the removal of castor and olive oils from rough tubes using air as flushant.

ternal) surface area of 19.48 cm^2. One tube was tunnel etched for 23 seconds, and the second was etched for 50 seconds. Following the etching, the lacquer was completely removed by immersion in a xylenes/methanol solution in an ultrasonic cleaner.

Once roughened and cleaned, the tubes underwent the exact oil cleaning procedure described previously. As before, castor and olive oils were used as the contaminant films.

Experimental Results

Figure 6 shows the combined data for the removal of castor and olive oils using air as the flushant and three tubes of 0.2-cm radii, but of differing surface roughness. As before, the data are plotted in the form $(1/\epsilon - 1)$ vs. t^*. The straight line represents the cleaning theory given by Eq. 19, but with a coefficient of 0.59 instead of the approximate value 0.807. It is noted that for each tube, the simple theory holds true for short dimensionless times, less than about 50 for tube #1, but less than 1 for tube #3 (corresponding to thicker films), and then levels off such that no further oil can be removed. The top leveling curve represents the data for the original untreated tube #1, having a natural surface roughness. The second leveling curve fits the data for rough tube sample #2 (tunnel etched for 23 seconds), and the last curve fits the data for rough tube sample #3 (etched for 50 seconds). It is noted that the longer the tube was etched (that is, the rougher the surface), the sooner the curve levels. In other words, the smoothest tube (#1) shows the highest degree of cleaning whereas the roughest tube (#3) shows the lowest degree of cleaning. For the removal of olive and castor oils, taken as combined data, the untreated tube levels at a $(1/\epsilon - 1)$ value of 57 ± 15 (26%). Tube #2 levels at 12 ± 3 (25%), and tube #3 levels at 3.4 ± 0.8 (24%). These leveling values were determined by statistically averaging all values of $(1/\epsilon - 1)$ obtained for t^* greater than 50. The corresponding standard deviation is also stated. These values of $(1/\epsilon - 1)$ correspond to a final film thickness, H_∞, of $1.6 \times 10^{-5} \pm 5.9 \times 10^{-6}$ cm (37%) for tube #1, $8.7 \times 10^{-5} \pm 2.7 \times 10^{-5}$ cm (31%) for tube #2, and $3.9 \times 10^{-4} \pm 1.3 \times 10^{-4}$ cm (33%) for tube #3.

With the values of the final film thicknesses known, it is of interest to have some measure of the surface roughness to see if the two quantities are of the same order of magnitude. If they are, then this is a good indication that surface roughness *is*, in fact, the limiting factor responsible for the leveling of the curves and the breakdown of the simple cleaning theory. As was explained earlier, a Bendix QB-type profilometer with a LK2-1520 probe was used to perform roughness measurements on the inside surface of each cylindrical tube. It should be noted that the profilometer probe can only enter about an inch into the tube. Thus, roughness measurements were taken down a 1-in. (25.4-mm) length inside each tube starting at several circumferential points near the inlet and outlet. The tubes ranged from 15.5 to 22.8 cm in total length.

The measured surface roughness amplitude value of each tube was chosen as the maximum of all observed values. The maximum was chosen on the presumption that the largest measurable surface disturbances are those most responsible for hindering or trapping the oil flow. The magnitude of the maximum surface roughness amplitude, δ_{max}, was 1.27×10^{-5} cm for tube #1, 6.35×10^{-5} cm for tube #2, and 1.27×10^{-4} cm for tube #3. Comparing these values to the final film thickness of each tube respectively, it is seen that both are of the same order of magnitude—of order 10^{-5} cm for tubes #1 and #2, and order 10^{-4} cm for the roughest tube #3. For simplicity and reference, the data presented here have been put into tabulated form (Table 2).

Interpretation of Results Based on Theory for Flow Over Rough Surfaces

An analysis of the results of the previous section suggests several interesting points. First, the cleaning model given by Eq. 19 holds true for short flushing times (thicker films) for all of the cases studied. Moreover, for both of the oils tested, the roughened tubes consistently yielded a lower leveling point (smaller fraction removed) than the untreated original tube. In fact, the roughest tube (#3) showed the lowest leveling point, followed by tube #2, and finally the untreated tube (#1). This result would suggest that it is easier to clean a "smooth" tube than a rough one, a result which is not surprising.

The fact that roughness can retard film removal was discussed previously, notably in the works of Higdon (1985),

Table 2. Data for Surface Roughness and Final Film Thickness Measurements

Tube	δ_{max}	Castor & Olive Oils
No. 1	1.27×10^{-5} cm	$(1/\epsilon - 1) = 57 \pm 15$ (26%) $H_\infty = 1.6 \times 10^{-5} \pm 5.9 \times 10^{-6}$ cm (37%)
No. 2	6.35×10^{-5} cm	$(1/\epsilon - 1) = 12 \pm 3$ (25%) $H_\infty = 8.7 \times 10^{-5} \pm 2.7 \times 10^{-5}$ cm (31%)
No. 3	1.27×10^{-4} cm	$(1/\epsilon - 1) = 3.4 \pm 0.8$ (24%) $H_\infty = 3.9 \times 10^{-4} \pm 1.3 \times 10^{-4}$ cm (33%)

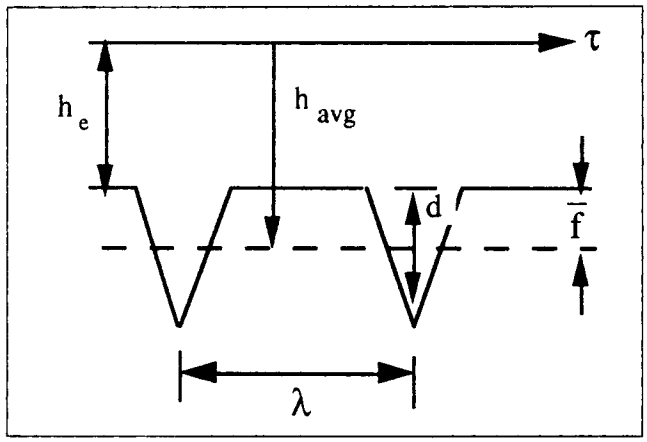

Figure 7. "Cavitylike" surface.

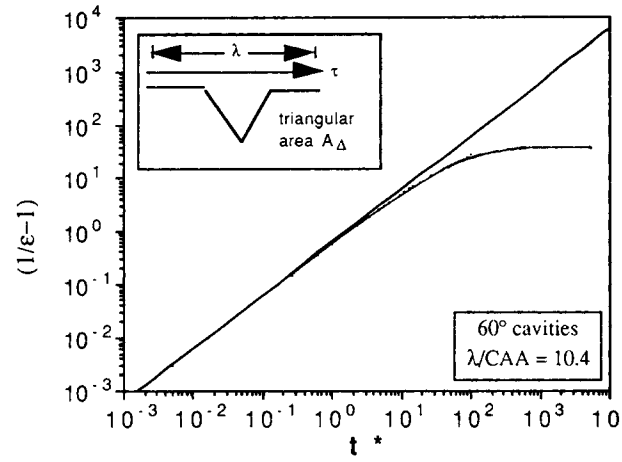

Figure 8. Numerical prediction of the effect of roughness on cleaning for constant shear stress and periodically-spaced triangular cavities.

Pozrikidis (1987), Yeckel et al. (1990), and Mickaily et al. (1992). The idea can be verified further by recasting the numerical results of Mickaily et al. (1992) in the form of Eq. 18. For example, their situation of pure drag flow over periodic two-dimensional 60° cavities with $\lambda/CAA = 10.4$ is chosen arbitrarily, where λ is the wavelength of the period, and CAA is the center average amplitude (see Figure 7 for definition of parameters). The film thinning parameter ϵ is here calculated based on the concept that all of the fluid within the cavity remains trapped. Hence, ϵ is calculated as:

$$\epsilon = \frac{h_e\lambda + A_\Delta}{H_o\lambda + A_\Delta} = \frac{\dfrac{h_e}{H_o} + \dfrac{A_\Delta}{\lambda H_o}}{1 + \dfrac{A_\Delta}{\lambda H_o}} \tag{22}$$

where A_Δ is the area of the triangular cavity holding the fluid, and h_e and λ are as defined in Figure 7. It is recalled that ϵ was defined as $\overline{H}/H_o$, where $\overline{H}$ is an average or equivalent film thickness determined experimentally. Here, however, ϵ is based on the actual film thickness h_e. As before, H_o is the initial film thickness, chosen arbitrarily for the simulations. For this particular numerical case study, $\lambda = 13.9$, $A_\Delta = 5.2$, and $CAA = 2A_\Delta/\lambda$. In the limit of $h_e/H_o \to 0$, or zero film thickness,

$$\epsilon = \frac{A_\Delta}{H_o\lambda + A_\Delta} \tag{23}$$

which means that all of the fluid is trapped within the cavity and corresponds to the leveling point where no further oil can be removed.

The dimensionless time parameter for a rough surface may be reformulated following the derivation of the cleaning model shown earlier. The average film velocity, previously defined by Eq. 1, is now reduced by a factor due to roughness. This factor is assumed to be the same as the flow reduction factor $\Re$ calculated by Mickaily et al. (1992) and given by:

$$\Re = Q_{\text{rough}}/Q_{h_e} \tag{24}$$

Note that the basis for $\Re$ is h_e rather than h_{avg}. Using these facts, we may write the average velocity as follows:

$$V_f = \frac{\tau_o H \Re}{2\mu_{\text{oil}}} \tag{25}$$

Returning to the derivation of the film-thinning model, we now find a new expression for the dimensionless flushing time, which accounts for tube roughness. Specifically,

$$0.59 = \int_1^{\epsilon} \frac{d(\overline{H}/H_o)}{(\overline{H}/H_o)^2 \Re(\overline{H}/H_o)} \tag{26}$$

Now, new values of t^* may be calculated by numerically integrating the righthand side of Eq. 26, using the flow reduction factor $\Re$ calculated by Mickaily et al. (1992). Figure 8 shows the results for the example geometry. The straight line represents the cleaning theory for a smooth surface. The curve indicates the numerical results for the rough tube. It is noted that when the film has been thinned to the level of roughness, the rate of film removal begins to level off. For this particular geometry, the leveling asymptotically approaches a value of $(1/\epsilon - 1)$ equal to 40, corresponding to fluid completely trapped below the cavity surface. The point to be noted here is not only that the limitation to film removal can be predicted numerically, but also that different geometrical roughnesses yield different limiting values of $(1/\epsilon - 1)$. This observation is consistent with the data shown in Figures 4 and 6.

Conclusions

In the course of this work, it has been shown that the simple hydrodynamic model given by Eq. 19 (with an empirically determined coefficient) may be used to describe the cleaning rate of a contaminant film from the inside of a tube for films thicker than the order of the surface roughness (or for smooth tubes). Furthermore, it has been demonstrated both experimentally and numerically that surface roughness limits the rate of the hydrodynamic cleaning process, presumably because of recirculation/retention in the rough architecture of the surface. The numerical simulations performed by Mickaily et al. (1992)

for shear flow over periodic cavitylike disturbances were recast to verify this concept.

As discussed in the Introduction, high levels of cleaning are required for many industrial applications. Cleaning of fuel feed lines and chemical, food or pharmaceutical production pipes are among a few examples. The hydrodynamic cleaning process developed in this work provides the basis for a feasible and environmentally sound alternative to solvent use. It has been shown that high fractions of oil contaminants can be removed simply by using a turbulent flow of a benign immiscible fluid, such as air. Moreover, it is important to recognize the generality of the hydrodynamic model given by Eq. 19 in that it may be used equally to predict the rate of aqueous cleaning. The model developed here may be used as long as the core fluid is immiscible with respect to the contaminant. Even though hydrodynamic cleaning does have limitations, it can be used in conjunction with other methods such as ultrasonic cleaning, evaporation, and dissolution to reduce the amount of solvent presently used in industrial practice.

Although this article discusses hydrodynamic cleaning and its limitations in detail, it is by no means an exhaustive study of the complex problems which occur during cleaning. For example, Herzstock (1990) achieved promising cleaning results by flushing with supercritical CO_2. He obtained 96% cleaning of complex geometries, such as oil-laden steel wool. In his study, two cleaning mechanisms occur simultaneously—one is hydrodynamic shear and the other is dissolution. In the supercritical phase, a gas has both shear and solubilizing capabilities on the contaminant film. This solventlike feature overcomes the limitation due to roughness observed for pure hydrodynamic cleaning.

Another interesting illustration of combined driving mechanisms for cleaning is the introduction of a surfactant into a flushant fluid such as water. In this case, hydrodynamics would dominate in the thick-film regime, whereas surface interactions would become important as the film thins. In the thin-film situation, the surfactant could potentially produce oil-enclosing micelles which would be flushed away by the mainstream flow. This characteristic also surmounts the roughness limitation to some degree. This enhanced cleaning situation provides an interesting direction for future studies.

Acknowledgment

Part of this work was carried out under fellowship support of the Alcoa Foundation. Support from the Space Science Division of General Dynamics Corporation is gratefully acknowledged, with special thanks to Charles Kropp and Michelle Won. Thanks also to Ray Merewether of RDI Instruments for providing the Bendix profilometer and measurement assistance. Discussions with our colleague, Dr. Joe Goddard, helped clarify our thinking and correct an error in the formulation of the hydrodynamic cleaning model.

Notation

A_Δ = area of triangular cavity, cm^2
CAA = center-average amplitude defined here as equal to $2A_\Delta/\lambda$, cm
f = Fanning friction factor for flushant fluid
$\bar{f}$ = mean of the surface function over the wavelength λ, cm
h_{avg} = average or equivalent channel height, cm
h_e = absolute channel height, cm
$\underline{H}$ = film thickness at any time t, cm
H = average film thickness at anytime t, cm
H_o = initial film thickness, cm
L = tube length, cm
Q = flushant flow rate, cm^3/s
Q_{h_e} = numerically determined flow rate for smooth surface with h_e channel height basis, cm^3/s
Q_{rough} = numerically determined flow rate for rough surface, cm^3/s
R = tube radius, cm
$\Re$ = dimensionless flow reduction factor
Re = Reynolds number
t^* = dimensionless flushing time
t_e = flushing time, s
V_f = average velocity in the oil film, cm/s
V_s = velocity at the oil/flushant interface, cm/s

Greek letters

δ_{max} = maximum profilometer measured surface roughness amplitude for a given sample, cm
ϵ = dimensionless film thinning parameter, ratio of film thickness at any time to the initial film thickness
$(1/\epsilon - 1)$ = limiting value of the dimensionless film thinning parameter for long flushing times
θ_c = contact angle of the oil on aluminum
ρ = density of the flushant, g/cm^3
σ = surface tension of the oil in air, dyne/cm
τ_o = shear stress at the oil/flushant interface, $dyne/cm^2$
λ = wavelength in the horizontal x-direction, cm
λ/CAA = dimensionless parameter defining intrinsic roughness of a surface
μ_{oil} = viscosity of the oil, $g/cm \cdot s$

Literature Cited

Alkire, R. C., H. Deligianni, and J-B Ju, "Effect of Fluid Flow on Convective Transport in Small Cavities," *J. Electrochem. Soc.*, **137**, 818 (1990).

Alwitt, R. S., H. Uchi, T. R. Beck, and R. C. Alkire, "Electrochemical Tunnel Etching of Aluminum," *J. Electrochem Soc.*, **131**, 13 (1984).

Evanoff, S., "Hazardous Waste Reduction in the Aerospace Industry," *Chem. Eng. Prog.*, **86**(4), 51 (1990).

Herzstock, J. J., "Cleaning With Supercritical CO_2," *NASA Tech. Briefs*, **14**(12), 58 (1990).

Higdon, J. J. L., "Stokes Flow in Arbitrary 2-Dimensional Domains: Shear Flow over Ridges and Cavities," *J. Fluid Mech.*, **159**, 195 (1985).

Higdon, J. J. L., "Effect of Pressure Gradients on Stokes Flow Over Cavities," *Phys. Fluids A*, **2**, 112 (1990).

Hu, H., and D. Joseph, "Lubricated Pipelining: Stability of Core-Annular Flow: II," *J. Fluid Mech.*, **205**, 359 (1989).

Israelachvili, J. N., and S. J. Kott, "Shear Properties and Structure of Simple Liquids in Molecularly Thin Films: The Transition from Bulk (Continuum) to Molecular Behavior with Decreasing Film Thickness," *J. Colloid Interf. Sci.*, **129**, 461 (1989).

Joseph, D., M. Renardy, and Y. Renardy, "Instability of the Flow of Two Immiscible Liquids with Different Viscosities in a Pipe," *J. Fluid Mech.*, **141**, 309 (1984).

Klepikov, E. S., and E. A. Kamener, "Tangential Action of a Flow of Liquid in the Removal of Thin Oil Films from Flat Surfaces," *Res. in Surf. Forces*, **3**, 372 (1971).

Mickaily, E. S., S. Middleman, and M. Allen, "Viscous Flow over Periodic Surfaces," *Chem. Eng. Comm.*, **117**, 401 (1992).

Middleman, S., "The Effect of Induced Air-Flow on Spin Coating of Viscous Liquids," *J. Appl. Phys.*, **62**, 2530 (1987).

Papageorgiou, D. T., C. Maldarelli, and D. S. Rumschitzki, "Nonlinear Interfacial Stability of Core-annular Film Flows," *Phys. Fluids A*, **2**, 340 (1990).

Pozrikidis, C., "Creeping Flow in a 2-D Channels," *J. Fluid Mech.*, **180**, 495 (1987).

Pozrikidis, C., "The Flow of a Liquid Film Along a Periodic Wall," *J. Fluid Mech.*, **188**, 275 (1988).

Preziosi, L., K. Chen, and D. Joseph, "Lubricated Pipelining: Stability of Core-Annular Flow," *J. Fluid Mech.*, **201**, 323 (1989).
Ruckenstein, E., and R. Jain, "Spontaneous Rupture of Thin Liquid Films," *Farad. Trans.*, **70**, 132 (1974).
Sharma, A., and E. Ruckenstein, "Mechanism of Tear Film Rupture and Formulation of Dry Spots on Cornea," *J. Colloid Interf. Sci.*, **106**, 12 (1985).
Strong, L., and S. Middleman, "Lubricant Retention on a Spinning Disk," *AIChE J.*, **35**, 1753 (1989).
Sullivan, T., and S. Middleman, "Factors that Affect Uniformity of Plating of Through-Holes in Printed Circuit Boards: I. Stagnant Fluid in the Through-Holes," *J. Electrochem. Soc.*, **132**, 1050 (1985).
Sullivan, T., S. Middleman, and R. Keunings, "Use of a Finite-Element Method to Interpret Rheological Effects in Blade Coating," *AIChE J.*, **33**, 2047 (1987).
Teletzke, G. F., H. T. Davis, and L. E. Scriven, "How Liquids Spread on Solids," *Chem. Eng. Commun.*, **55**, 41 (1987).
Wolf, K., "Ozone Depletion and the Use of CFCs," *J. Environ. Sci.*, **32**, 41 (1989).
Yeckel, A., and S. Middleman, "Removal of a Viscous Film from a Rigid Plane Surface by an Impinging Liquid Jet," *Chem. Eng. Commun.*, **50**, 155 (1987).
Yeckel, A., S. Middleman, and L. Klumb, "The Removal of Thin Liquid Films from Periodically Grooved Surfaces by an Impinging Jet," *Chem. Eng. Comm.*, **96**, 69 (1990).

Manuscript received Jan. 21, 1993, and revision received Mar. 15, 1993.